

Study of neutrino-nucleus interaction at around 1 GeV using  
a 3D grid-structure neutrino detector, WAGASCI at J-PARC  
neutrino monitor hall

A. Bonnemaison, R. Cornat, L. Domine, O. Drapier, O. Ferreira, F. Gastaldi,  
M. Gonin, J. Imber, M. Licciardi, F. Magniette, T. Mueller, L. Vignoli, and O. Volcy

*Ecole Polytechnique, IN2P3-CNRS, Laboratoire Leprince-Ringuet, Palaiseau,  
France*

S. Cao and T. Kobayashi

*High Energy Accelerator Research Organization (KEK), Tsukuba, Ibaraki, Japan*

M. Khabibullin, A. Khotjantsev, A. Kostin, Y. Kudenko, A. Mefodiev, O. Mineev,  
S. Suvorov, and N. Yershov

*Institute for Nuclear Research of the Russian Academy of Sciences, Moscow, Russia*

B. Quilain

*Kavli Institute for the Physics and Mathematics of the Universe (WPI), The  
University of Tokyo Institutes for Advanced Study, University of Tokyo, Kashiwa,  
Chiba, Japan*

T. Hayashino, A. Hiramoto, A.K. Ichikawa, K. Nakamura, T. Nakaya, K Yasutome,  
and K. Yoshida

*Kyoto University, Department of Physics, Kyoto, Japan*

Y. Azuma, J. Harada, T. Inoue, K. Kin, N. Kukita, S. Tanaka, Y. Seiya,  
K. Wakamatsu, and K. Yamamoto

*Osaka City University, Department of Physics, Osaka, Japan*

A. Blondel, F. Cadoux, Y. Karadzhov, Y. Favere, E. Noah, L. Nicola, S. Parsa, and  
M. Rayner

*University of Geneva, Section de Physique, DPNC, Geneva, Switzerland*

N. Chikuma, F. Hosomi, T. Koga, R. Tamura, and M. Yokoyama

*University of Tokyo, Department of Physics, Tokyo, Japan*

Y. Hayato

*University of Tokyo, Institute for Cosmic Ray Research, Kamioka Observatory,  
Kamioka, Japan*

Y. Asada, K. Matsushita, A. Minamino, K. Okamoto, and D. Yamaguchi

*Yokoyama National University, Faculty of Engineering, Yokoyama, Japan*

December 5, 2017

## 1 Introduction

The understanding of neutrino-nucleus interactions in the 1 GeV energy region is critical for the success of accelerator-based neutrino oscillation experiments such as the T2K experiment. Complicated multi-body effects of nuclei render this understanding difficult. The T2K near detectors have been measuring these and significant progress has been achieved. However, the understanding is still limited. One of the big factors preventing from full understanding is the non-monochromatic neutrino beam spectrum. Measurements with different but some overlapping beam spectra would greatly benefit to resolve the contribution from different neutrino energies. We, the Wagasci collaboration, proposes to study the neutrino-nucleus interaction at the B2 floor of the neutrino monitor building, where different neutrino spectra can be obtained due to the different off-axis position. Our experimental setup contains 3D grid-structure plastic-scintillator detectors filled with water as the neturino interaction target (Wagasci modules), two side- and one downstream- muon range detectors(MRD's). The 3D grid-structure and side-MRD's allows a measuremen of wider-angle scattering than the T2K off-axis near detector (ND280). High water to scitillator material ratio enables the measurement of the neutrino interaction on water, which is higly desired for the T2K experiment because it's far detector, Super-Kamiokande, is composed

of water. The MRD's consist of plastic scintillators and iron plates. The downstream-MRD, so called the Baby MIND detector, is also work as a magnet and provides the charge identification capability. The charge identification is essentially important to select antineutrino events in the antineutrino beam because contamination of the neutrino events is as high as 30%. Most of the detectors has been already constructed and commissioned as the J-PARC T59 experiment. Therefore, the collaboration will be ready to proceed to the physics data daking for the T2K beam time in January 2019. We will provide the cross sections of the charged current neutrino and antineutrino interactions on water with slightly higher neutrino energy than T2K ND280 with wide angler acceptance. When combined with ND280 measurements, our measurement would greatly improve the understanding of the neutrino interaction at around 1 GeV and contribute to reduce the most significant uncertainty of the T2K experiment.

## 2 Experimental Setup

Figure. 1 shows a schematic view of the entire set of detectors. A central detector, Wagasci modules, consists of 3D grid-structure plastic-scintillator detectors filled with water as the neturino interaction target. They are surrounded by two side- and one downstream- muon range detectors(MRD's) The MRD's are used to select muon tracks from the charged-current (CC) interactions and to reject short tracks caused by neutral particles that originate mainly from neutrino interactions in material surrounding the central detector, like the walls of the detector hall, neutrons and gammas, or neutral-current (NC) interactions. The muon momentum can be reconstructed from its range inside the detector. The MRD's consist of plastic scintillators and iron plates. In addition, eaco of the iron plates of the downstream-MRD, so called the Baby MIND detector, is wound by a coil and can be magnetized. It provide the charge selection capability.

For all detectors, scintillation light in the scintillator bar is collected and transported to a photodetector with a wavelength shifting fiber (WLS fiber). The light is read out by a photodetector, Multi-Pixel Photon Counter (MPPC), attached to one end of the WLS fiber. The signal from the MPPC is read out by the dedicated electronics developed for the test experiment to enable bunch separation in the beam spill. The readout electronics is triggered using the beam-timing signal from MR to synchronize to the beam. The beam-timing signal is branched from those for T2K, and will not cause any effect on the T2K data taking.

T2K adopted the off-axis beam method, in which the neutrino beam is intentionally directed 2.5 degrees away from SK producing a narrowband  $\nu_\mu$  beam. The off-axis near detector, ND280, is installed towards the SK direction in the B1 floor of the near detector hall of the J-PARC neutrino beam-line. We propose to install our detector in the B2 floor of the near detector hall, where the off-axis angle is similar but slightly different. The candidate detector position in the B2 floor is shown in Fig. 2. The expected neutrino

tmp.pdf

Figure 1: Schematic view of entire sets of detectors.

energy spectrum at the candidate position is shown in Fig. 3.

## 2.1 Wagasci module

The dimension of the central detector is  $100\text{cm} \times 100\text{cm}$  in the x and y directions and  $200\text{cm}$  along the beam direction. The total water and hydrocarbon masses serving as neutrino targets are  $\sim 1$  ton each. Inside the central detector, plastic scintillator bars are aligned as a 3D grid-like structure, shown in Fig. 4, and spaces in the structure are filled with the neutrino target materials, water and hydrocarbon. When neutrinos interact with hydrogen, oxygen or carbon, in water and hydrocarbon, charged particles are generated. Neutrino interactions are identified by detecting tracks of charged particles through plastic scintillation bars. Thanks to the 3 D grid-like structure of the scintillator bars, the central detector has  $4\pi$  angular acceptance for charged particles. Furthermore, adopting a  $2.5\text{cm}$  grid spacing, short tracks originated from protons and charged pions can be reconstructed with high efficiency. Thin plastic scintillator bars (thickness  $\sim 0.3\text{cm}$ ) will be used for the central detector to reduce the mass ratio of scintillator bars to neutrino target materials, because neutrino interactions in the scintillator bars are a background for the cross section measurements. Scintillator bars whose dimensions are  $2.5\text{cm} \times 0.3\text{cm} \times 100\text{cm}$  will be used for the central detector. The total number of channels in the central detector is 12880.

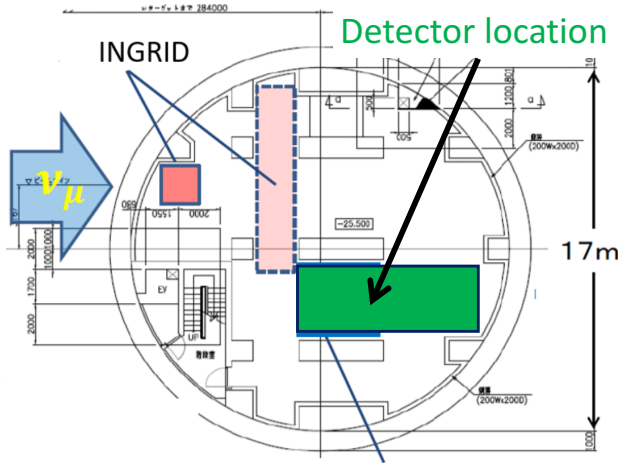


Figure 2: Candidate detector position in the B2 floor of the near detector hall.

## 2.2 Baby MIND

### 2.3 Side muon range detector

Two Side-MRD modules will be constructed by the end of January 2018. Each Side-MRD module is composed of iron plates and scintillator bars for tracking secondary particles from neutrino interactions. Support structure of the Side-MRD module mainly consists of 11 steel plates of which dimensions are  $1800 \times 1610 \times 30$  mm $^3$ , is sized as  $2236 \times 1630 \times 975$  mm $^3$  as shown in Fig. 5, and weights  $\sim 8.5$  ton. Scintillator bars were produced by Uniplast company in Vladimir, Russia. Each bar is polystyrene based and made by extrusion technology with scintillating composition of 1.5% PTP and 0.01% POPOP. Then each bar's surface is etched by a chemical agent to form a white diffuse layer. The usage of this method gives almost ideal contact between the scintillator and the reflector which allows us to gain in light yield up to 50% compared to clear scintillator. 80 scintillator bars are installed in one Side-MRD module, and each scintillator bar is sized as  $1800 \times 200 \times 7$  mm $^3$  including reflector part. Scintillation light is collected by wave length shifting fibers, Y-11 (S type) with a diameter of 1.0 mm produced by Kuraray. The fiber is glued by optical cement EJ-500 in a S-shape groove on the surface of the scintillator bar as shown in Fig. 6. Using this technique allows us to uniform light collection over scintillator's surfaces. Two optical connectors as shown in Fig. 7 are attached to either end of the fiber, and scintillation light is lead to two MPPCs, S13081-050CS(X1), produced at Hamamatsu Photonics. Optical connector of such type (so-called Baby-mind type of optical connector) consists of two parts (see Fig. 7): a) a MPPC cover and b) a ferrule. Ferrule b) is fixed in

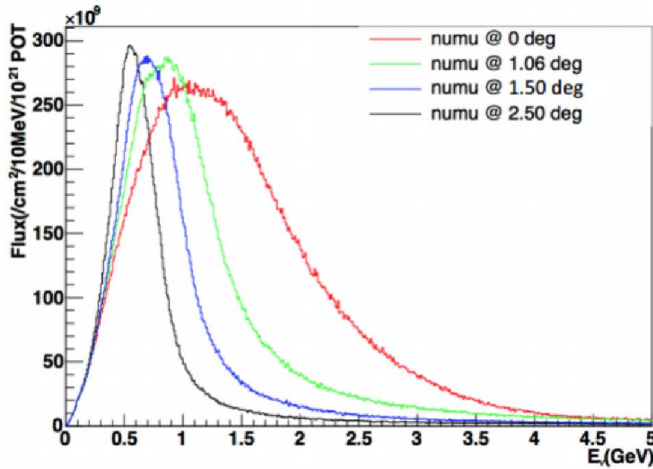


Figure 3: Neutrino energy spectrum at the candidate detector position(red). The spectrum at the ND280 site (black) is also shown.

scitillator by glue with glued fiber in it, cut by mill and polished to form an optical contact between the fiber end and the MPPC. Cover a) is clicked into place on ferrule b) and used to fix MPPC in optical contact. To ensure the tightness of the contact between the MPPC window and the fiber's end in ferrule a special spring made of sponge rubber is used (Fig. 8). For each MPPC, 667 pixels of APD are aligned in a shape of square 1.3 mm on a side.

Construction of scintillator bars of the Side-MRD modules had been completed at INR in Russia, and they were transported to Japan in July 2017. Before and after the shipping their perfomance were check with cosmic rays. The main mesured parameters were light yield and light yield assymetry. For the light yields  $LY_1$  and  $LY_2$  at counter's two ends correspondent assymetry is calculated as  $100\% \times \frac{LY_1 - LY_2}{LY_1 + LY_2}$ . Thus at INR we selected 324 counters from total 332 produced with mean light yield of 45 p.e./MIP and assymetry less than 10 % at the center of the bar. When counters arrived to Japan their perfomance were checked once again at Yokohama National University. In the bench setup here two small trigger counters were put in the center of measured bars. Trigger signal is the coincidence between top and bottom trigger counters made of  $NaI(Tl)$  crystals of  $6 \times 6 \times 17 cm^3$  size. Average total light yield obtained in the central part of the scintillator slab is 40 p.e./MIP and varies from 32 to 50 p.e./MIP. (Fig. 9 (left)). Only two counters here showed relatively high assymetry close to 25 % as shown in Fig. 9 (right). By such quality assurance tests of the counters we selected 320 scintillator bars to be installed in four Side-MRD modules. In addition, for four counters there were measured time resolution for single and combination of the counters. For one counter time resolution defined as uncertainty on  $(T_{left} - T_{right})/2$

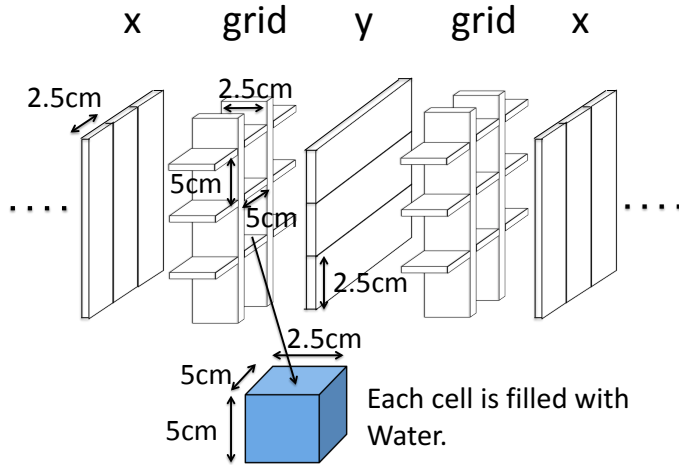


Figure 4: Schematic view of 3D grid-like structure of plastic scintillator bars inside the central detector.

was obtained  $\sigma = 1\text{ns}$  (Upper left plot in Fig. 10). Further, for a set of  $n$  counters combined time resolution will be  $\frac{(T_L-T_R)_1+(T_L-T_R)_2+\dots+(T_L-T_R)_n}{2\times n}$ . The result of combination of 2,3,4 counters is 0.79 ns, 0.66 ns and 0.68 ns accordingly (Fig. 10).

Construction of Side-MRD modules will be done from November 2017 to January 2018 at Yokohama National University, then they will be transported to J-PARC and will be installed to the B2 floor of the T2K near detector hall before staring the T2K beam in March 2018.

### 3 Physics goals

We will measure the differential cross section for the charged current interaction on  $\text{H}_2\text{O}$  and/or  $\text{CH}$ . The water-scintillator mass ratio of the Wagasci module is as high as 5:1 and the high purity measurement of the cross section on  $\text{H}_2\text{O}$  is possible. One experimental option is to replace one of the two Wagasci module with the T2K proton module which is fully made with plastic scintillators. It will allow the precise comparison of cross section between  $\text{H}_2\text{O}$  and  $\text{CH}$  and also comparison of cross sections with ND280. Another option is to remove water from one of the two Wagasci module. The water-out WAGASCI module will make it possible to measure wider- angle scatterings for  $\text{CH}$  target and will provide a low density medium for the detection of low momentum protons. The water-out WAGASCI data also can be used to subtract the background from interaction with scintillators in the water target measurement . Our setup would allow the measurements of inclusive and

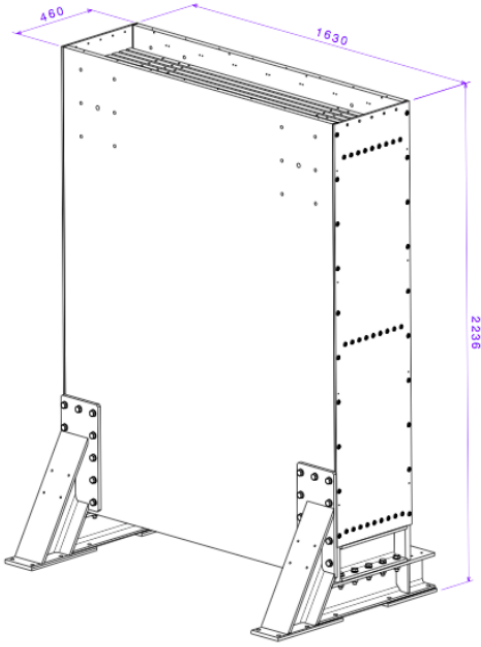


Figure 5: Support structure of the Side-MRD module.

also exclusive channels such as  $1-\mu$ ,  $1-\mu 1p$ ,  $1-\mu 1\pi \pm np$  samples, former two of which are mainly caused by the quasi-elastic and  $2p2h$  interaction and the latter is mainly caused by resonant or coherent pion production and deep elastic scattering. In general, an accelerator produced neutrino beam spectrum is wide and the energy reconstruction somehow rely on the neutrino interaction model. Therefore, recent neutrino cross section measurement results including T2K are given as a flux-integrated cross section rather than cross sections as a function of the neutrino energy to avoid the model dependency. We can provide the flux-averaged cross section. In addition, by combining our measurements with those at ND280, model-independent extraction of the cross section for narrow energy region becomes possible. This method was demonstrated in ?? and also proposed by P\*\* (NUPRISM).   
add Yasutome plot here or later.

### 3.1 Expected number of events

Expected number of neutrino events after the event selections is evaluated with Monte Carlo simulations as we will discuss in Section 6.  $2.41 \times 10^4$  CC events are expected in two WAGASCI modules after the selection with  $1 \times 10^{20}$  POT in neutrino-mode, and its purity is 75.5 %. In case we choose the option with one WAGASCI module and the T2K

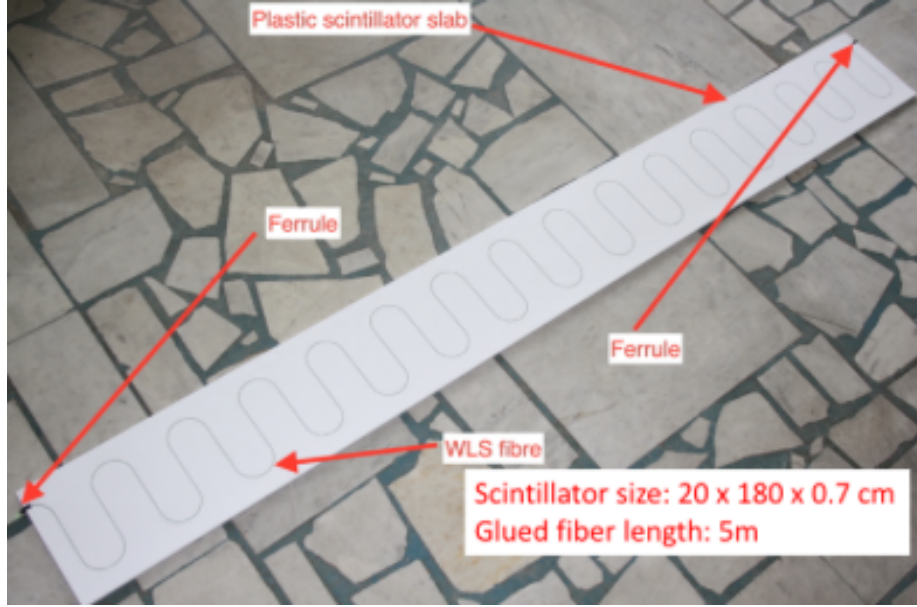


Figure 6: Scintillator bar of the Side-MRD modules.

proton module,  $1.2 \times 10^4$  CC events are expected in the WAGASCI module and  $\sim 1 \times 10^4$  CC events are expected in the T2K proton module. In case we choose the option with one water-in WAGASCI module and one water-out WAGASCI module,  $1.2 \times 10^4$  CC events are expected in the water-in module and  $0.24 \times 10^4$  CC events are expected in the water-out module.

### 3.2 Nuclear effects

In T2K experiment, neutrinos interact with bound nucleons in relatively heavy nuclei (Carbon and Oxygen), so the cross-section is largely affected by nuclear effects. The nuclear effects are categorized as nucleons' momentum distribution in nucleus, interactions with correlated pairs of nucleons in nucleus (two particles-two holes, 2p2h), collective nuclear effects calculated with Random Phase Approximation (RPA) and final state interactions (FSI) of secondary particles in the nuclei after the initial neutrino interactions.

The 2p2h interactions mainly happen through  $\Delta$  resonance interactions following a pion-less decay and interactions with a correlated nucleon pair. The 2p2h interactions are observed in electron scattering experiments (add ref. here) where the 2p2h events observed in the gap between Quasi-Elastic region and Pion-production region as shown in Fig. ??.

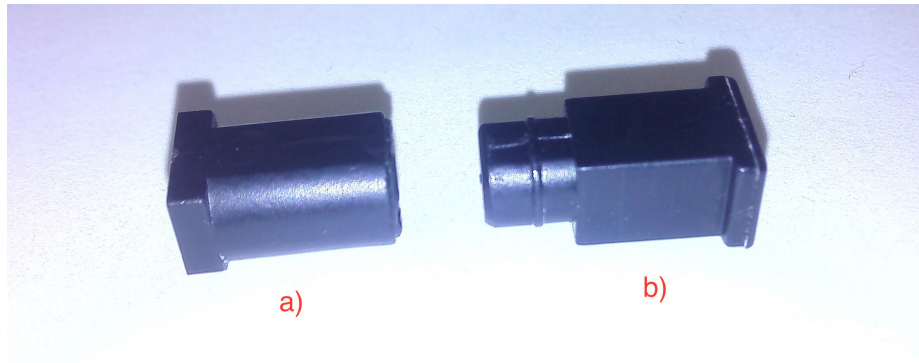


Figure 7: Optical connector for the Side-MRD scintillator. a) MPPC cover. b) Ferrule.

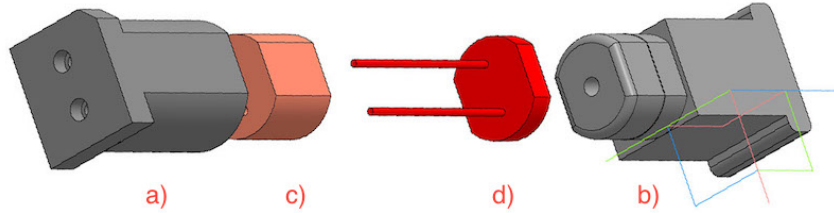


Figure 8: Scheme of the MPPC placement in optical connector. a) MPPC cover. b) Ferrule. c) Spring (sponge rubber). d) MPPC.

Neutrino experiments also attempt to measure the 2p2h interactions, but separation of the QE peak and the 2p2h peak is more difficult because transferred momentum ( $p$ ) and energy ( $w$ ) are largely affected by neutrino energies which cannot be determined event-by-event in the wide energy spectrum of the accelerator neutrino beam. Our model-independent narrow neutrino spectra extracted from combined analyses of our data and ND280 data are ideal for searching the 2p2h interaction because clearer separation of the QE peak and the 2p2h peak is expected. Another way to observe the 2p2h interaction is direct measurement of proton tracks in CC0 $\pi$  sample with low detection threshold and full acceptance. Fig. ?? shows proton multiplicities in CCQE events and 2p2h events, and Fig. ?? shows opening angles among two proton tracks in the same samples. The water-out WAGASCI can provide good sample for the 2p2h interaction search because its low density medium enables the detection of low momentum protons in addition to the full acceptance.

The corrections from collective nuclear effects calculated by RPA as a function of  $Q^2$  are shown in Fig. ???. The  $Q^2$  dependence of the correction can be tested by measuring angular

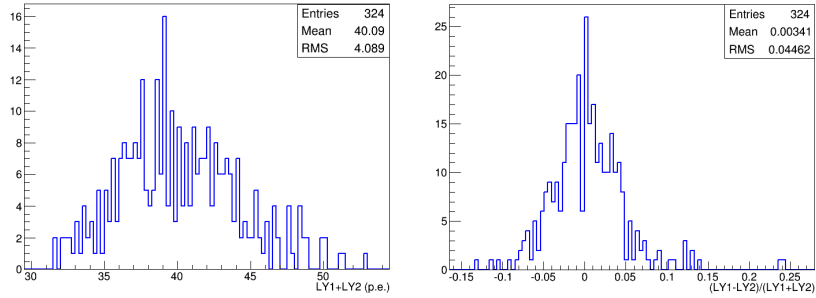


Figure 9: Total light yield distribution (left) and light yield assymetry (right) measured at YNU.

distribution of muons in CC1- $\mu$  and CC1- $\mu 1p$  events. The uncertainties of the corrections in low (high)  $Q^2$  regions can be constrained by observing the events with a forward-going (high-angle) muon, so it is essential to measure muon tracks with full acceptance.

T2K experiment is starting to use  $\nu_e$  CC1 $\pi$  events for its CP violation search to increase the statistics. One of the biggest uncertainty of the CC1 $\pi$  sample comes from the final state interactions of pions in the nuclei after the initial neutrino interactions because they change the multiplicity, charge and kinematics of the pions. The multi-pion production events can be migrated into the CC1 $\pi$  sample due to the FSIs, and they become important backgrounds. We can constrain the uncertainties from the pion FSIs by measuring pion rescattering in the detector and pion multiplicity in  $\nu_\mu$  CCn $\pi$  sample with low detection threshold and full acceptance for pion tracks. The water-out WAGASCI can provide good sample for the pion FSI studies because its low density medium enables the detection of low momentum pions in addition to the full acceptance.

## 4 Status of J-PARC T59 experiment

We had submitted a proposal of a test experiment to test a new detector with a water target, WAGASCI, at the T2K near detector hall to J-PARC PAC on April 2014, and the proposal was approved as J-PARC T59. There are several updates on the project after three years from then. Fist, the start time of neutrino beam measurement is changed from December 2015 to October 2017, and the requested neutrino beam is changed from  $1 \times 10^{21}$  POT of  $\nu$  beam to  $0.8 \times 10^{21}$  POT of anti- $\nu$  beam. Second, the detector configuration is changed. In the original proposal, central neutrino detector are expected to be surrounded by newly developed muon-range detectors (MRDs), but we will use spare neutrino detectors of the T2K experiment instead of them during neutrino beam measurement from October to December 2017. Construction of the newly developed MRDs, Baby-MIND and Side-

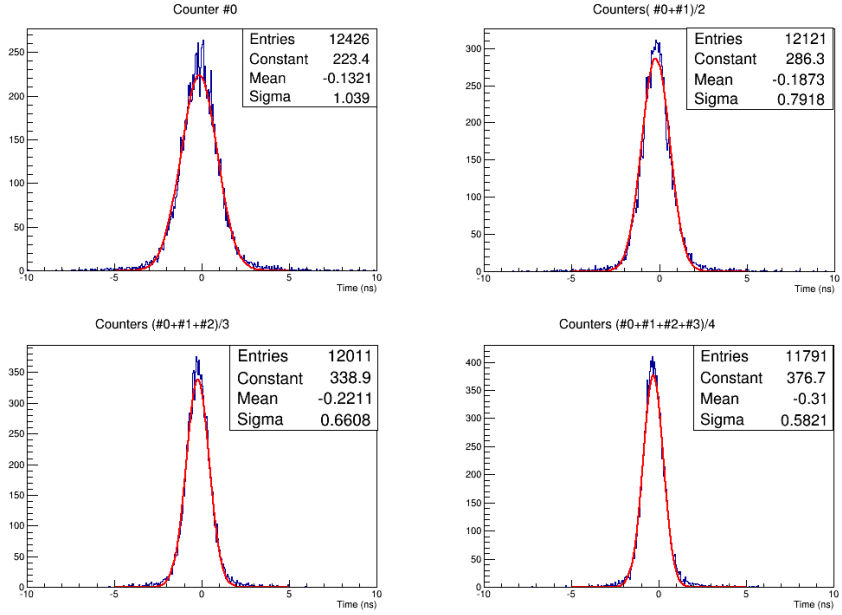


Figure 10: Time resolution for one (upper left) and a set of 2,3,4 Side-MRD counters.

MRD, is in progress, and they will be installed to the both sides and the downstream of the central neutrino detector from January to March 2018. Then, we will resume neutrino beam measurements from March 2018 and will take the neutrino beam data until May 2018.

#### 4.1 On-axis beam measurement with Prototype detector

Add INGRID water module measurement here.

#### 4.2 Plans from October 2017 to May 2018

J-PARC MR will extract its proton beam to T2K neutrino beam-line from October to December 2017, and, from March to May 2018. T2K experiment will produce anti-neutrino beam and will accumulate  $\sim 8 \times 10^{20}$  POT data during the above period.

J-PARC T59 will perform neutrino beam measurements on the B2 floor of the T2K near neutrino detector hall during the above period to test basic performances of the WAGASCI detector and new electronics. During the beam measurements from October to December 2017, one WAGASCI module will be placed between spare neutrino detectors of the T2K experiment, INGRID Proton module and INGRID standard module. Here, the INGRID Proton module is used as a charged particle VETO detector and, the INGRID

standard module is used as a downstream muon detector. We had submitted a proposal to use these spare neutrino detectors for the T59 neutrino beam measurements to the T2K collaboration, and we got an approval from T2K.

During the beam measurements from March to May 2018, Baby-MIND and two side muon-range detector (Side-MRD) modules will be installed on the downstream and the both sides of the WAGASCI detector, as shown in Fig. 11, to increase angular acceptance for secondary charged particles from neutrino interactions. Add Baby-MIND commissioning items here!!!

tmp.pdf

Figure 11: J-PARC T59 detector configuration with Baby-MIND and two Side-MRD modules from Mar. to May 2018. (Need to prepare the figure.)

Expected number of neutrino events in the WAGASCI detector during the above beam period is evaluated with Monte Carlo simulations. Neutrino beam flux at the detector location is simulated by T2K neutrino flux generator, JNUBEAM, neutrino interactions with target materials are simulated by a neutrino interaction simulator, NEUT, detector responses are simulated using GEANT4-based simulation. The neutrino flux at the detector location, 1.5 degrees away from the J-PARC neutrino beam axis, is shown in Figure 3, and its mean neutrino energy is around 0.68 GeV. An event display of the GEANT4-based detector simulation is shown in Figure 14.

To perform the detector performance test, the following event selections are applied to the data. First, track reconstructions are performed in the WAGASCI detector, and the reconstructed vertex is required to be inside a defined fiducial volume,  $80 \times 80 \times 32 \text{ cm}^3$  region at the center of the detector, to reduce contamination from external backgrounds. Second, at least one charged particle is required to reach to INGRID standard module

or Side-MRD modules, and it makes more than two hits in these sub-detectors. With the event selection, expected numbers of the neutrino-candidate events during the beam period are summarized in Table 1. Using the data, we will test the detector performance with  $\sim 3\%$  statistical uncertainties.

## 5 Detector performance

### 5.1 Wagasci module

To demonstrate the performance of the Wagasci module and also to study the neutrino interaction, the first Wagasci module was installed at the on-axis position, in front of the T2K INGRID horizontal center module in 2016. The INGRID module is made of iron plates and segmented plastic scintillator bars. It's cross sectional size viewed from the beam direction is  $1\text{ m} \times 1\text{ m}$ . The charged current interactions in the Wagasci module are selected by requiring a muon track candidate in the INGRID modules. Here, we describe the performance of the Wagasci module evaluated at this T2K on-axis measurement. Figure 12 shows the light yeild of channels for muons produced by the interaction of neutrinos in the hall wall. The light yield is sufficiently hgh to get good hit efficieincy. A track search

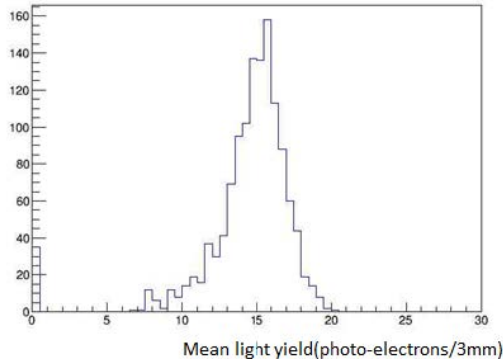


Figure 12: Light yield of channels for muons produced by the interaction of neutrinos in the hall wall.

algorithm based on the cellular automaton has been developed using the software tools by the T2K INGRID. The tracking efficiency in 2-dimentional projected plane was evalualted by comparing the reconstructed track in the Wagasci module and the INGRID module and shown in Fig.13. Note that that the tracking efficinecy for high angle ( $> 70\text{ deg}$ ) is not evaluated because of the acceptance of the INGRID module, not because of the limitation of the Wagasci module.

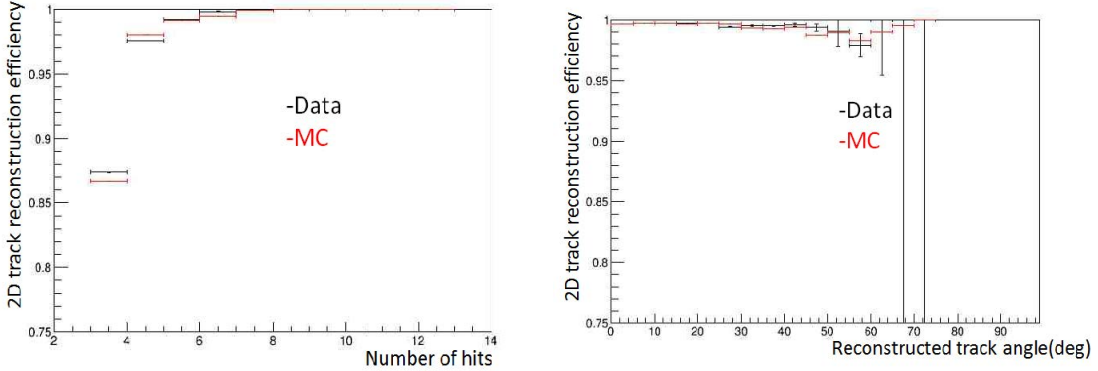


Figure 13: 2D track reconstruction efficiency as a function of number of hits (left) and track angle (right). Here the track angle is the one reconstructed by the INGRID module.

## 5.2 Baby MIND

## 5.3 Side muon range detector

## 6 MC studies

### 6.1 Detector simulation

Expected number of neutrino events in the WAGASCI detector is evaluated with Monte Carlo simulations. Neutrino beam flux at the detector location is simulated by T2K neutrino flux generator, JNUBEAM, neutrino interactions with target materials are simulated by a neutrino interaction simulator, NEUT, detector responses are simulated using GEANT4-based simulation. The neutrino flux at the detector location, 1.5 degrees away from the J-PARC neutrino beam axis, is shown in Figure 3, and its mean neutrino energy is around 0.68 GeV.

#### 6.1.1 Detector geometry

The detector geometry in the GEANT4-based simulation is slightly different from the actual detector as shown in Fig. 16. The active neutrino target region consists of four WAGASCI modules, and each WAGASCI detector has the dimension with 100 cm  $\times$  100 cm in the x and y directions and 50 cm along the beam direction. An event display of a MC event in the WAGASCI detectors is shown in Figure ???. Two Side-MRD modules are installed at both sides of the WAGASCI modules, and each Side-MRD module consists of ten iron plates whose dimension is 3 cm (thickness)  $\times$  180 cm (height)  $\times$  320 cm (width). The distance between the Side-MRD modules and WAGASCI modules is 60 cm. The

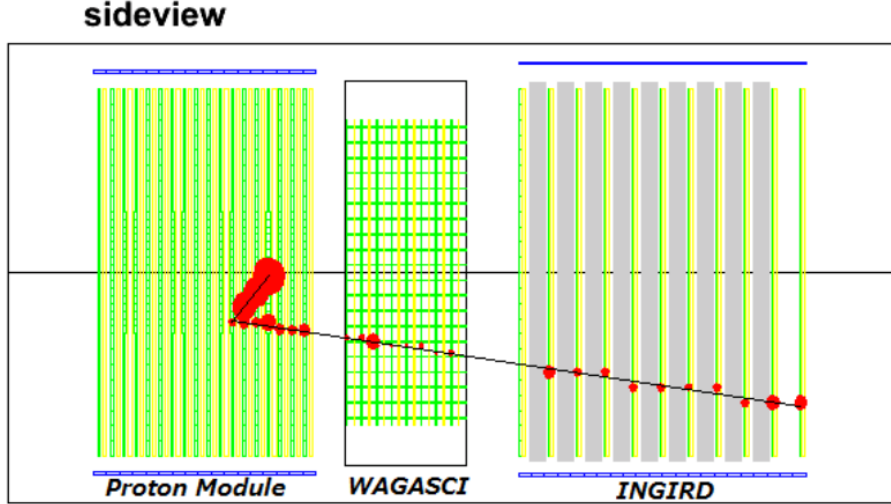


Figure 14: J-PARC T59 event display of a neutrino event in the GENAT4-based detector simulation.

downstream-MRD equivalent to the Baby-MIND is installed at the downstream of the WAGASCI modules. The downstream-MRD consists of ten iron plates whose dimension is 3 cm (thickness)  $\times$  180 cm (height)  $\times$  320 cm (width) and another ten iron plates whose dimension is 6 cm (thickness)  $\times$  180 cm (height)  $\times$  320 cm (width). The distance between the downstream-MRD modules and WAGASCI modules is 60 cm.

In order to estimate backgrounds from neutrino interactions in the wall and floor of the experimental hall, the geometry of the experimental hall is implemented in the GEANT4-based detector simulation.

### 6.1.2 Response of detector components

The energy deposit inside the scintillator is converted into the number of photons. The effects of collection and attenuation of the light in the scintillator and the WLS fiber are simulated, and the MPPC response is also taken into account. The light yield is smeared according to statistical fluctuations and electrical noise.

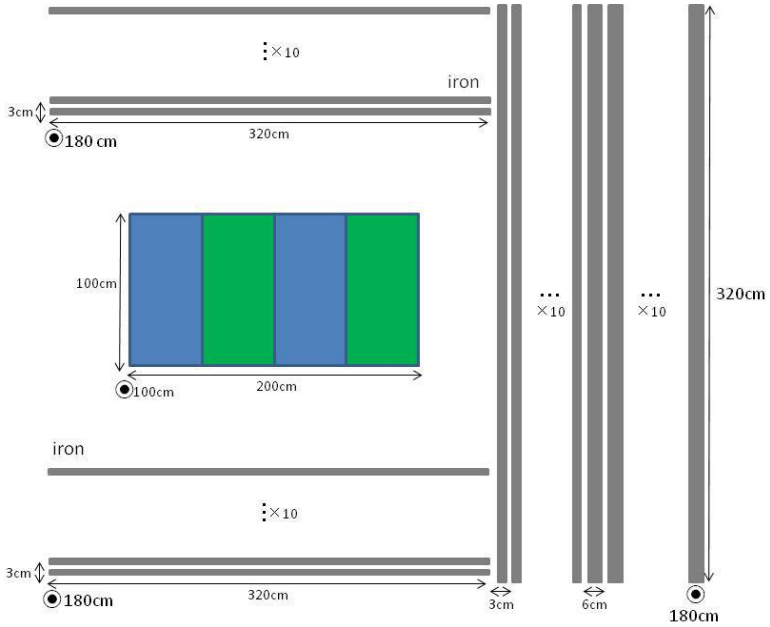


Figure 15: Geometry of the detectors in the Monte Carlo simulation.

## 6.2 Track reconstruction

To select neutrino interaction from the hit patterns, a track reconstruction algorithm is developed. The flow of the track reconstruction is as follows.

1. Two-dimensional track reconstruction in each sub-detectors
2. Track matching among the sub-detectors
3. Three -dimensional track reconstruction

Add explanation about two-dim reco, track matching and three-dim reco here.

## 6.3 Event selection

The events with the track which starts in 5 cm from the wall of the WAGASCI module are rejected to remove the background from the outside as shown in Fig. 17.

To reject backgrounds from NC and neutral particles, the longest tracks are required to penetrate more than one (five) iron plates in Side-MRD modules (Baby-MIND) as shown in Figure 18. In order to measure muon momentum, the longest tracks are required to stop in MRDs (Side-MRD modules and Baby-MIND) or penetrate all iron plates.

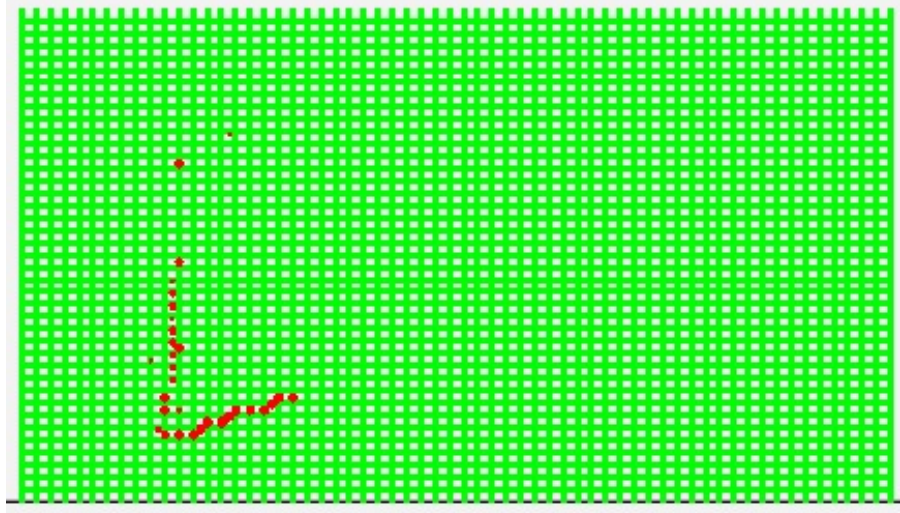


Figure 16: An event display of MC event in WAGASCI detectors. Green lines are scintillators and red circles are the hit channels.

#### 6.4 Selected events

Table 1 shows numbers of the selected events after each event election.  $2.41 \times 10^4$  CC events are expected with  $1 \times 10^{21}$  POT in neutrino-mode, and the purity is 75.5 %. The main background is the neutrino interaction in the scintillators inside the WAGASCI detector.

Table 1: Expected number of the neutrino-candidate events in two WAGASCI modules after the event selections with  $1 \times 10^{21}$  POT in neutrino-mode.

Cut	CC	NC	BG (Scinti.)	BG (outside)	
Track reconst.	$6.27 \times 10^4$	$3.61 \times 10^3$	$1.62 \times 10^4$	$1.04 \times 10^6$	$1.12 \times 10^6$
Fiducial	$3.95 \times 10^4$	$1.75 \times 10^3$	$9.71 \times 10^3$	$7.32 \times 10^3$	$5.55 \times 10^4$
Penetrated iron	$3.02 \times 10^4$	$9.12 \times 10^2$	$7.67 \times 10^3$	$2.04 \times 10^3$	$4.00 \times 10^4$
Stop in MRDs	$2.41 \times 10^4$	$8.65 \times 10^2$	$6.19 \times 10^3$	$1.64 \times 10^3$	$3.19 \times 10^4$
after all cuts	75.5 %	2.71 %	19.4 %	5.14 %	100 %

Figure 19 shows the reconstructed angles of the longest tracks in the selected events. Figure 20 shows differences between true angles and the reconstructed angles of the longest tracks in the selected events, and the angle resolution is  $\sim 3$  degrees.

Figure 21 shows the iron plane numbers corresponding to the end points of the longest tracks in the selected events.

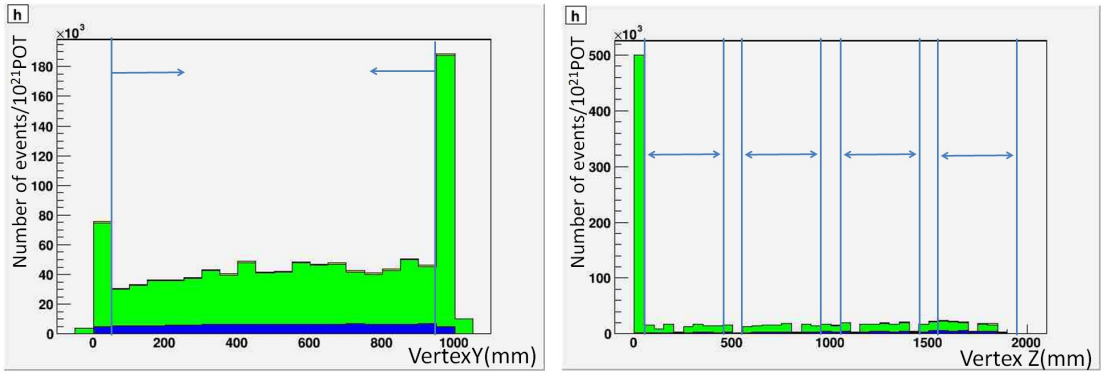


Figure 17: Event selection with the vertex of the track. Blue hist. are events from the WAGASCI modules, green hist. are events from the experimental hall, and yellow hist. are events from the Side-MRD modules and the downstream-MRD.

Table 2 shows particles which produce the longest tracks in the selected events, and the fraction of muons is 85.6%.

Table 2: Particles which produce the longest tracks in the selected events.

particles	fraction
$\mu$	85.6%
$\pi^+, \pi^-$	4.8%
p	4.3%
$e^+, e^-$	4.5%

Figure 22 shows detection efficiencies of muon tracks in the selected events as a function of muon's true angle and true momentum. The efficiency in the large angle region is low because Side-MRD modules only cover sides of the WAGASCI modules. The efficiency in the low momentum region is also low because more than two hits are required to reconstruct the track in the WAGASCI detector.

## 6.5 Cross section measurements on water

In the water target events, the background from interaction with scintillators has to be subtracted by using the measurement of the hydrocarbon target.

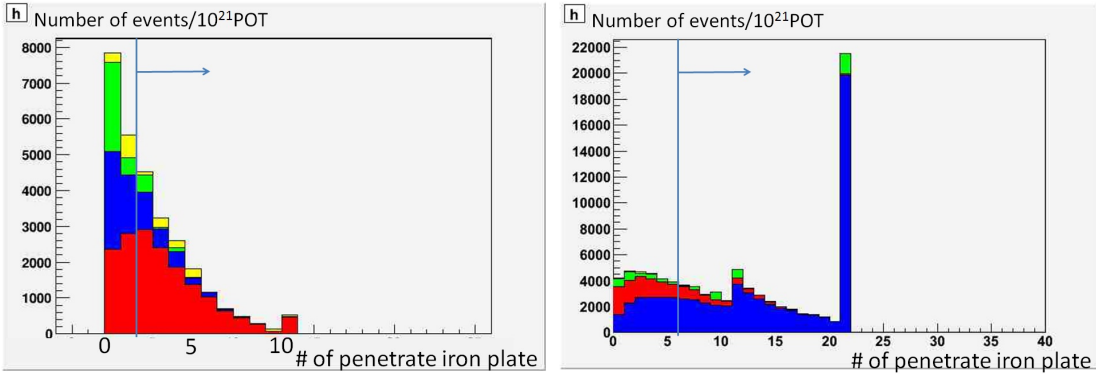


Figure 18: Event selection with the number of the penetrated iron plates in the Side-MRD modules (left) and the Baby-MIIND (right). Blue and red hist. are events from the WAGASCI modules, green hist. are events from the experimental hall, and yellow hist. are events from the Side-MRD modules and the Baby-MIIND.

#### 6.5.1 Charged current cross section measurement

## 7 Standalone WAGASCI-module performances

In the previous sections, the WAGASCI detector was studied using the Muon Range Detectors. In this section, the standalone abilities of WAGASCI module are presented. Using the WAGASCI configuration presented in Section 6, we have evaluated that only 7% of the muons will be stopped in one of the WAGASCI modules. THowever, this proportion increases to 53% for pions and 73% for protons produced by neutrino interactions at  $1.5^\circ$  off-axis. Figure 23 shows the momentum distribution of these daughter particles as well as for the sub-sample stopped in one of the WAGASCI modules. Therefore, the study of the standalone abilities of the WAGASCI module in this section are dominantly motivated by:

- the accurate measurement of the neutrino interaction final states. Though most of the muons will be reconstructed and identified in the MRDs, the hadronic particles will predominantly stops in one WAGASCI module. One has therefore to rely exclusively on the WAGASCI module information alone to reconstruct, identify and measure the momentum of pions or protons.
- the coverage of the MRDs is not  $4\pi$ . Using the WAGASCI module information can therefore help to constraint the particles that exits the WAGASCI module but do not geometrically enters any MRD.
- the particle identification of low momenta muons  $p_\mu < 300 \text{ MeV}/c$  that will leave only few hits in the MRD. Using the WAGASCI module information will clearly enhance

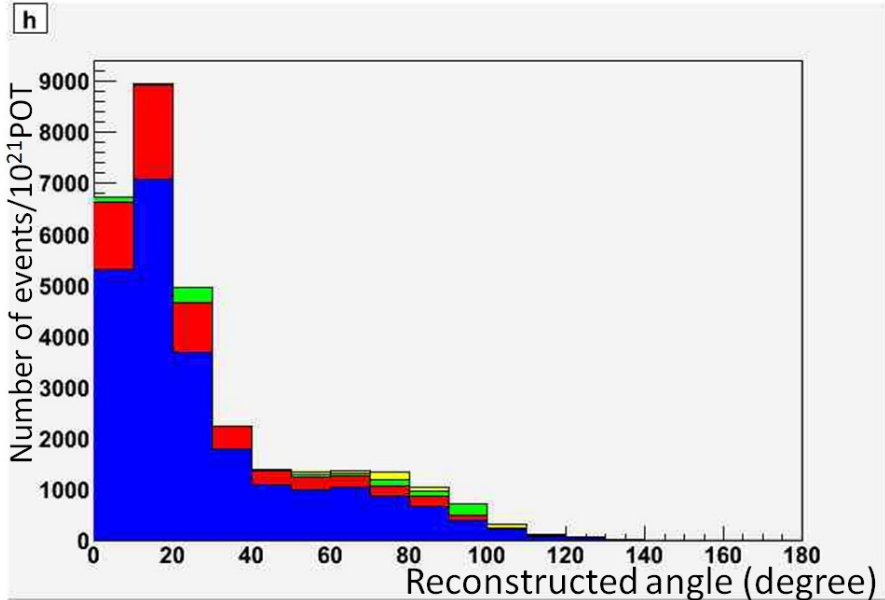


Figure 19: The reconstructed angles of the longest tracks in the selected events. Blue and red hist. are events from water and scintillators in the WAGASCI modules, green hist. are events from the experimental hall, and yellow hist. are events from the Side-MRD modules and the Baby-MIND.

the particle identification.

This study is based on an original study done for the ND280 upgrade target, with some modifications. Though the cell size is similar to the WAGASCI configuration presented in Section 6, the external dimensions are different ( $186.4 \times 60 \times 130$  cm $^3$ ). Whenever the results are presented with this external size and this parameter is likely to impact the result, it will be mentioned.

Note that in this section, a simplified reconstruction algorithm presented in Section 7.1 is used. The fiducial volume is chosen accordingly as the inner cube of the module which surfaces are distant of  $4 \times$  scintillator space = 10 cm from the module external surfaces. The neutrino interactions are simulated using NEUT v5.3.2. The NEUT input neutrino flux is estimated using JnuBeam v13a and assuming the detector to be located at 1.5° off-axis, as in Section 6. Note that the event reconstruction efficiency as a function of true neutrino energy might be changed at 1.5°, due for example to different  $Q^2$  distributions. For this reason, one has to note that the reconstruction results might slightly be changed from 2.5° and 1.5°. To avoid a similar change on the particle-only reconstruction efficiencies, they will be presented as a function of variables that completely characterize the particle

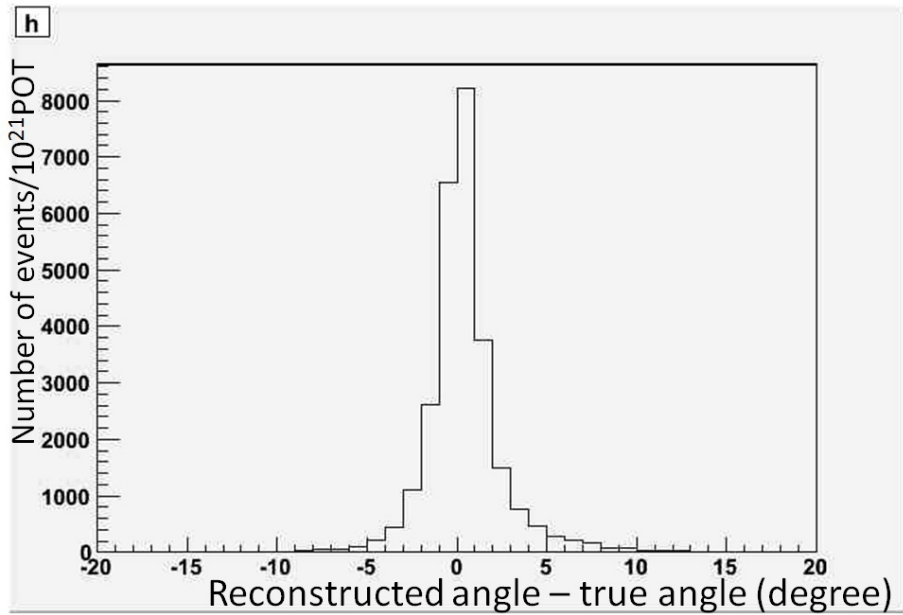


Figure 20: Differences between true angles and the reconstructed angles of the longest tracks in the selected events.

kinematic state, *i.e.* its momentum and angle. Figure 24 shows the vertices distributions of the daughter particles of neutrinos interacting one standard WAGASCI water-module. In this section, we will show the detector reconstruction and particle identification in this phase space, both for leptonic and hadronic particles. We will finally show an empty WAGASCI module can highly enhance the ability to constrain the neutrino interaction final state which is critical to reduce the corresponding uncertainties.

## 7.1 Reconstruction algorithm

### 7.1.1 Description

For this section, an ideal “simulated” reconstruction is developed. A particle is reconstructed if:

1. The particle is charged.
2. Lets at least one hit (energy deposit  $> 2.5$  photo-electron) in a scintillator.
3. The particle enters one TPC and let one hit in the tracker.  
Or

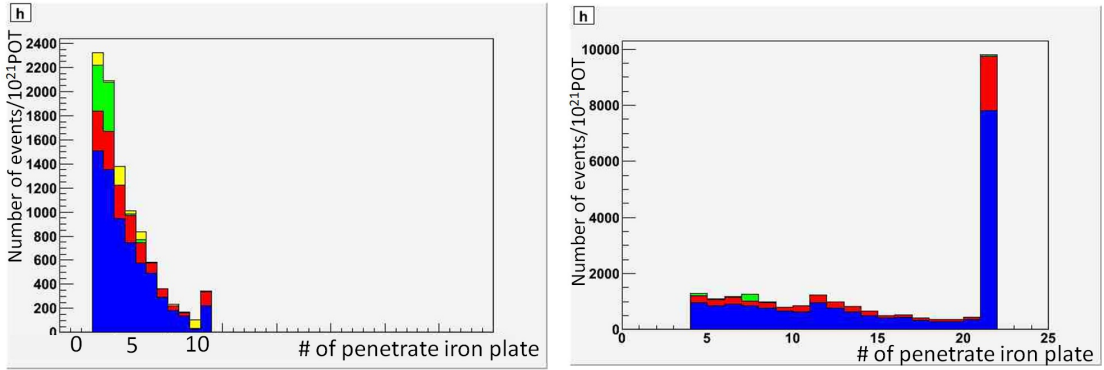


Figure 21: Iron plane numbers in Side-MRD (left) and Baby-MIND (right) corresponding to the end points of the longest tracks in the selected events. Blue and red hist. are events from water and scintillators in the WAGASCI modules, green hist. are events from the experimental hall, and yellow hist. are events from the Side-MRD modules and the Baby-MIND.

- The particle should be long enough to be reconstructed by the detector in at least 2 out of 3 views (XZ, YZ, XY). The length criterion requires the particle to let at least 4 hits in the detector. In the “less favourable case” of pure longitudinal or transverse going tracks, it represents a the track length of  $L_{track} \geq 4 \times \text{scintillator space} = 10.0 \text{ cm}$ .
- In the views where particles pass the length criterion, the particle shall not be superimposed with longer tracks in at least two views. The superposition criterion is estimated with the distance inter-tracks (DIT) which corresponds to the orthogonal distance between two tracks at the ending point of the shortest one (see Figure 25). For a track 1, the superposition criterion is tested with every longer tracks that starts at the same vertex. Let  $\vec{p}_1$  the vector of track 1, and  $p_1^a$  its projections in the XZ, YZ and XY planes respectively for  $i=1,2,3$ . Note that these are projections in a 2D planes and not on a direction vector. In this case, the relative angle between the track 1 and a longer track 2 (of vector  $\vec{p}_2$ ) in a view a is given by:

$$\cos \theta = \frac{\vec{p}_1^a \cdot \vec{p}_2^a}{\|\vec{p}_1^a\| \|\vec{p}_2^a\|} \quad (1)$$

and the distance inter track is given by:

$$\text{DIT} = \|\vec{p}_1^a\| \sin \theta \quad (2)$$

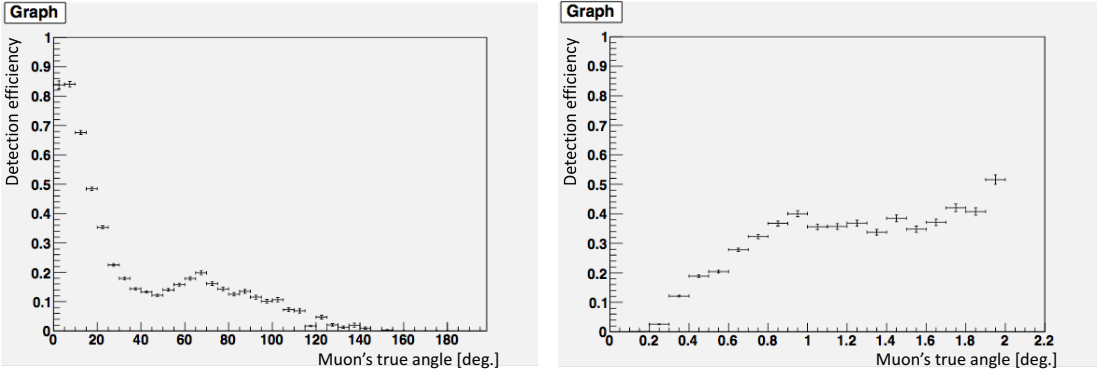


Figure 22: Detection efficiencies of muon tracks in the selected events as a function of muon's true angle (left) and true momentum (right).

The DIT should be higher than  $4 \times$  scintillator width for the track 1 to be not superimposed with the track 2 in the view a, which also corresponds to 10.0 cm in the nominal configuration.

### 7.1.2 Performances

The particle-only reconstruction efficiencies and the reconstruction threshold in momenta are shown in Table 3. This threshold is defined as the maximal momentum for which the reconstruction efficiency is smaller than 30%. The thresholds in muon and pion momenta are 150 MeV/c. Most of the muons are above this threshold (see Figure 24) which leads to a 79% reconstruction efficiency.

	$\mu$	$\pi$	p
Reconstruction Efficiency	79%	52%	26%
Momentum threshold	150 MeV/c	150 MeV/c	550 MeV/c

Table 3: Reconstruction efficiency and momentum threshold for muons, pions and protons. The threshold is defined as the maximal momentum for which particles have a reconstruction efficiency smaller than 30%.

The lower pion and proton efficiencies (respectively 52% and 26%) are due to lower efficiencies for similar momenta than muons, coming from strong interactions as shown on Figures 26. Efficiencies of each particle type tend to decrease in the backward region

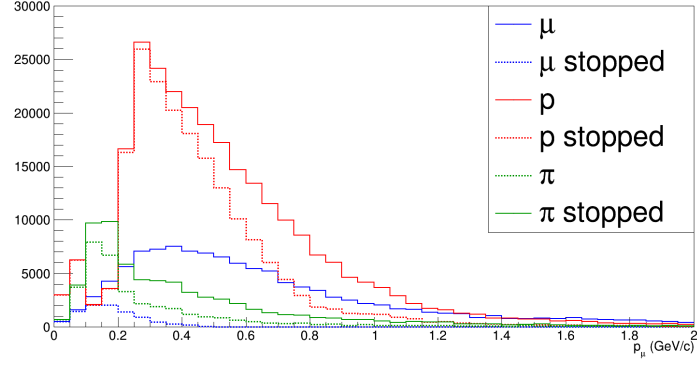


Figure 23: Momentum distribution of true particles in WAGASCI (plain) and corresponding distributions only for particles stopping into the WAGASCI module (dashed).

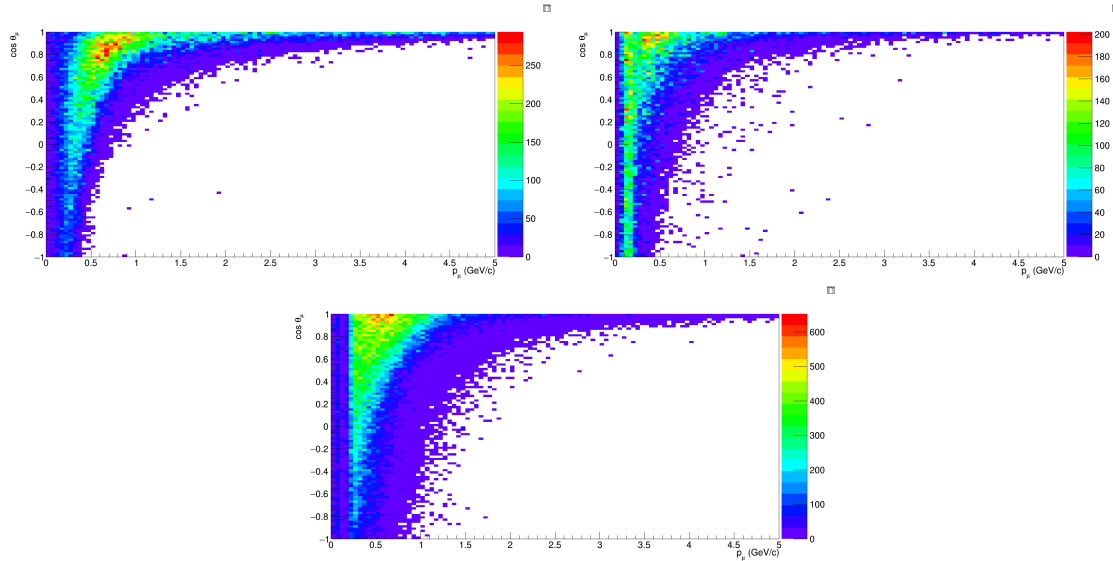


Figure 24: True number of muons (left), charged pions (right) and protons (bottom) in the two WAGASCI water-module as a function of the particles momenta and angles at  $1.5^\circ$ .

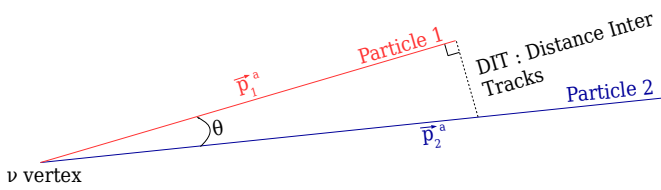


Figure 25: Definition of the distance inter tracks.

due to particle lower momenta. However, for a fixed momentum value, the reconstruction efficiency is almost uniform which confirms the ability of the WAGASCI detector to reconstruct high angle tracks.

The reconstruction is thereafter tested on neutrino events. Table 4 summarizes the number of reconstructed events and efficiencies for each interaction type. As expected from the high muon reconstruction efficiency, the charged current interactions have reconstruction efficiencies  $\geq 85\%$ .

	CC0π	CC1π	CCOthers	NC	All
Reconstruction efficiency	85%	87%	91%	22%	68%

Table 4: Number of true interactions reconstructed. The purity and reconstruction efficiency of each true interaction is also shown.

The reconstruction efficiencies as a function of the neutrino energy and muon kinematics are respectively shown on Figure 27 and 28.

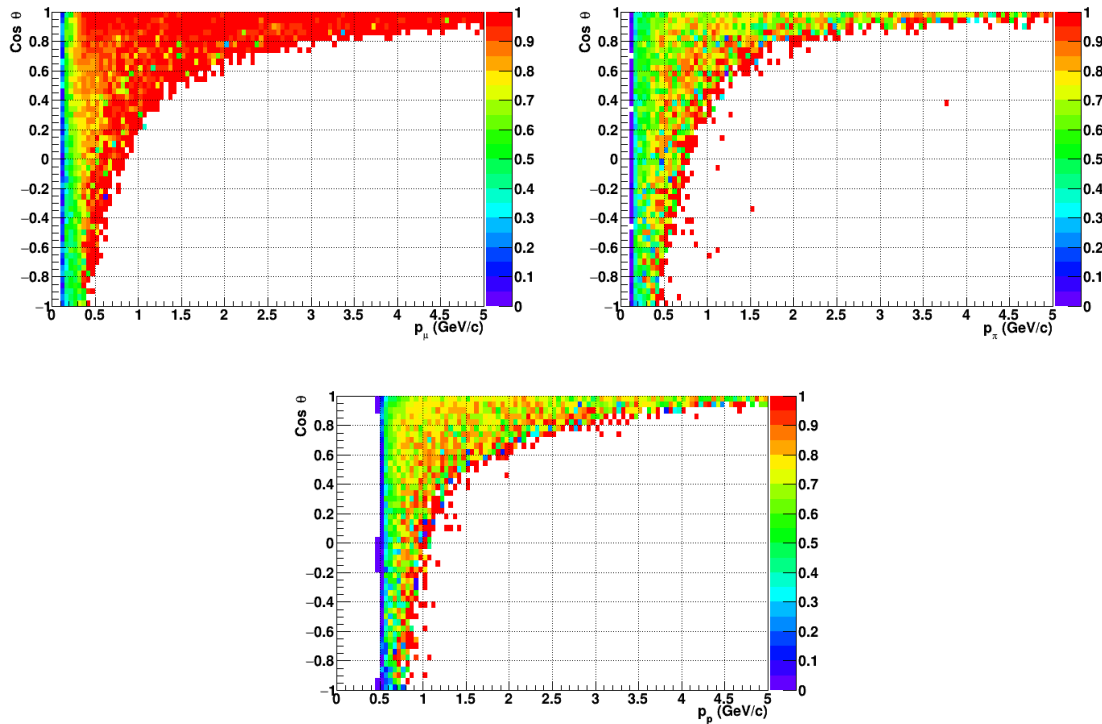


Figure 26: Reconstruction efficiency of muons (left), charged pions (right) and protons (bottom) in the WAGASCI water-module as a function of the particles momenta and angles.

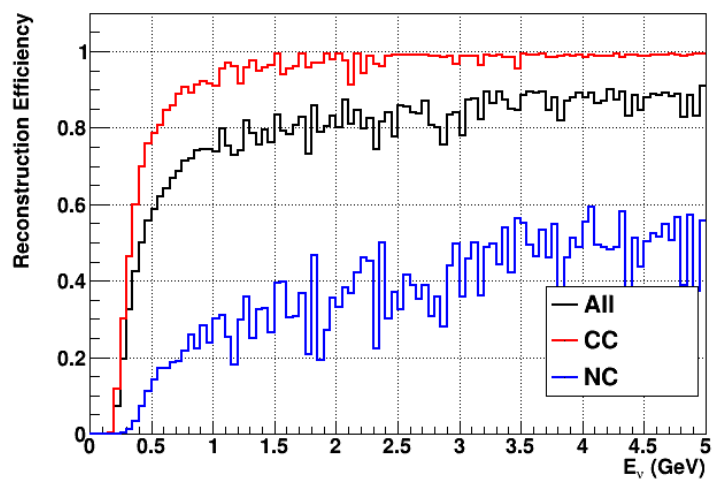


Figure 27: Reconstruction efficiency of all neutrino (black), CC (red) and NC (blue) interactions in the WAGASCI water-module as a function of the neutrino energy.

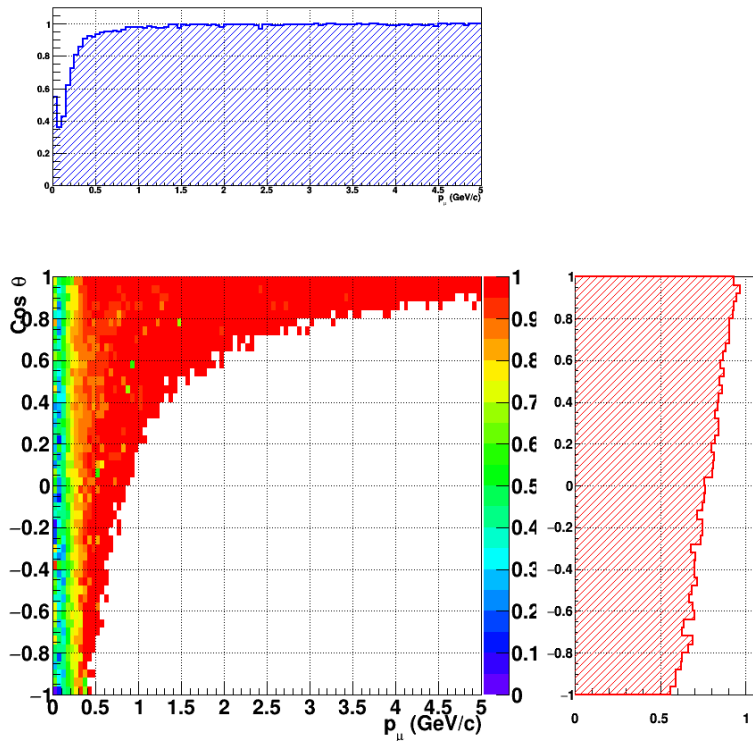


Figure 28: Reconstruction efficiency of CC interactions in the WAGASCI water-module as a function of the muon kinematic variables (momentum and angle).

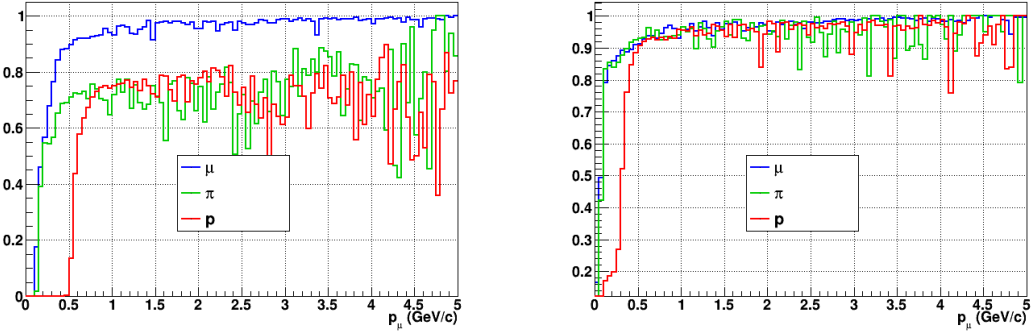


Figure 29: Reconstruction efficiency for muons, pions and protons in the water-in (left) and water-out (right) modules.

Note that a Particle Identification Algorithm has been also developed. It is based on the charge deposition of the particles in the scintillator, of the detection of a decay-electron. However, this information highly depends on the number of scintillator hit by a particle, which creates an important difference between a real WAGASCI module and the one used for the ND280-upgrade simulation. For this reason, the corresponding results will not be detailed here, but can be found in [?].

## 7.2 Background subtraction: the water-out module

In the nominal configuration, 20% of the neutrino interactions occurs on scintillators ( $C_8H_8$ ). This background should be removed in order to measure the neutrino interaction on the same target as Super-K, which suppress the differences in cross-section models. For this purpose, we propose to use a water-out module, where the water is replaced by air. The detector is therefore fully active and has a 3 mm spatial resolution (scintillator thickness) which create an ideal detector to reconstruct and identify hadrons, and study np-nh interactions. The counter-part is the difference in particle energy deposition between the water and this water-out module that will need to be corrected for. In this section, we present the capabilities of such a module, and the impact it can have on cross-section measurements for the neutrino community in general and T2K in particular.

The same reconstruction and selection as the water-in module is applied. Figure 29 shows the comparison between the water-in and the water-out reconstruction efficiencies for muon, pions and protons. 90% of the muons and 87% of the pions are reconstructed, while 70% of the protons are even reconstructed. It allows to lower down the proton threshold to 250 MeV/c (see Table 5).

As a consequence of tracking even low momenta particle, the reconstruction efficiency is uniform and almost maximal on the entire  $\cos \theta_\mu$  phase space, as shown on Figure 30.

	$\mu$	$\pi$	p
Reconstruction Efficiency	90%	87%	70%
Momentum threshold	50 MeV/c	50 MeV/c	250 MeV/c

Table 5: Reconstruction efficiency, proportions of  $\mu$ -like and non  $\mu$ -like and momentum threshold for muons, pions and protons in the empty module. The threshold is defined as the maximal momentum for which particles have a reconstruction efficiency smaller than 20%.

Since the fiducial mass represents 0.25 tons, the total number of events is divided by a factor of 3 compared to the water-in module. The water-out module offers interesting possibilities to study np-nh interaction since 70% of the protons are reconstructed. In the future, a possible separation as a function of the number of proton track will be studied. Moreover, we are currently pursuing the use of single and double transverse variables (cite Xianguo) to open new possibilities for separating np-nh from Final State Interactions, or for isolating the interactions on hydrogen from interactions on carbon in this module.

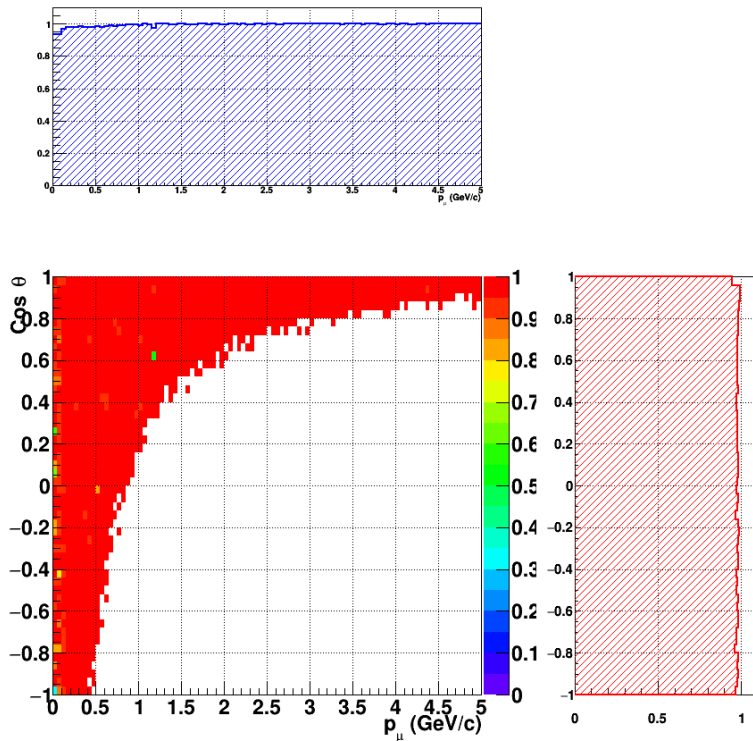


Figure 30: Reconstruction efficiency of CC interactions in the WAGASCI empty module as a function of the muon kinematic variables (momentum and angle).

## 8 Schedule

We would like to start a physics data taking from T2K beam time after the summer shutdown in 2018. By then, commissioning and tests of the detectors will be completed in J-PARC T59. The experiment can run parasitically with T2K, therefore we request no dedicated beam time nor beam condition as discussed in the following section.

Once the approved POT is accumulated, the WAGASCI modules will be removed from the experimental site, but we would like to keep the Baby-MIND and the Side-MRD modules on the B2 floor of the NM pit as common platforms of future neutrino experiments using the T2K neutrino beam.

## 9 Requests

### 9.1 Neutrino beam

The experiment can run parasitically with T2K, therefore we request no dedicated beam time nor beam condition. As data taking periods, we request the ‘nominal’ T2K one-year operation both for the neutrino beam and the antineutrino beam. The T2K has been requesting  $0.9 \times 10^{21}$  POT/year and actually accumulating about  $0.7 \times 10^{21}$  POT/year in recent years. For each year, starting from the Autumn, T2K is running predominantly in the neutrino mode or in the antineutrino mode. Our request is to have one-year neutrino-mode data and another one-year antineutrino mode data assuming that the POT for the fast extraction in each year is more than  $0.5 \times 10^{21}$  POT.

### 9.2 Equipment request including power line

We request the followings in terms of equipment on the B2 floor:

- Site for the WAGASCI modules, Side-MRD modules and BabyMIND and their electronics system on the B2 floor of the near detector hall (Fig. 2).
- Anchor points (holes) on the B2 floor to secure the WAGASCI modules, Side-MRD module and Baby-MIND (Fig. ??)
- Power line for the magnets in Baby-MIND: 400 V tri-phase 48-to-62 Hz, capable of delivering 12 kW.
- Electricity for electronics and water circulation system, 3 kW, standard Japanese electrical sockets.
  1. Online PCs: 2.1 kW
  2. Electronics: 0.7 kW
  3. Water sensors: ?

- Air conditioner for cooling heat generation at Baby-MIND magnets, online PCs and electoronics
- Beam timing signal and spill information
- Network connection

## 10 Conclusion